

Numerical Method to Obtain the Two-Dimensional Electronic States for Open Boundary Scattering Problems

Henry K. Harbury and Wolfgang Porod

*Department of Electrical Engineering
University of Notre Dame
Notre Dame, IN 46556*

Abstract

We discuss a numerical method for computing the electronic scattering states for a fully two-dimensional open boundary scattering domain. The scattering states may then be used to obtain the local electron density in the vicinity of the scatterers which is necessary for a numerical study of the residual resistivity dipole and the “electron wind” force relevant to electromigration. The scattering states may also be used to calculate the local electron density of states which has recently been directly imaged by STM experiments on the surface of copper. Our numerical method is based upon the partial wave expansion of the known asymptotic form of the wave-function on the solution domain boundary. The wave-function and the normal derivative are then matched on the boundary resulting in a linear system of equations.

I. Introduction

The large volume of recent literature on the study of electromigration increasingly emphasizes the importance of the local non-uniform fields near scattering centers. It is clear that a detailed understanding of the local fields near scatterers is needed to understand phenomena in which the residual resistivity dipole (RRD) [1-2] and Friedel-oscillations [3] play an important role. Such a local field treatment is used in the application of the Kubo linear-response formalism to compute the “electron wind” force experienced by a scatterer in electromigration [4-7].

The importance of local field effects near scattering centers is most clearly and elegantly demonstrated by the recently published scanning tunnelling microscope (STM) experiments performed on the Cu(111) surface by Crommie *et al.* [8-9]. In these experiments, the local density of states (LDOS) of the two-dimensional electron gas (2DEG) on the stepped surface of Cu(111) was directly probed by an STM tip at low temperature. The images of the LDOS revealed standing-wave patterns due to electron scattering from step edges and defects.

In this paper, a numerical method is presented in which the two-dimensional electronic

scattering states are obtained by solving the effective mass Schrödinger equation over a 2D domain with an open boundary. The method uses the partial wave expansion of the known asymptotic solution and matches the wave-function and its normal derivative on the boundary. The resulting system of linear equations can be solved by the finite element method. These scattering states may then be used to compute the electron density and the LDOS inside the scattering domain. A self-consistent treatment would require an iterative solution of scattering states using a Hartree potential [10].

The physical model for the partial wave expansion is presented in section II. Section III presents the finite element formulation of the problem. An example solution for a repulsive scatterer is presented in section IV. In conclusion, we summarize our method in Section V.

II. Model

We view electron transport in the spirit of Landauer's picture for the residual resistivity dipole (RRD) [1-2] in which the incident carrier flux is identified as the fundamental driving transport quantity in a "jellium" model with a background scattering time τ which gives rise to the bulk resistivity $\rho_0 = m^*/ne^2\tau$, where n is the electron density and m^* is the electron effective mass. As is schematically depicted in Fig. 1, the incident electron flux is elastically scattered by the defect, schematically shown as the shaded spot, and is partially transmitted and partially reflected. For the metallic "jellium" model, the problem domain is assumed to be in the ballistic regime and scattering is assumed to take place within the region close to the scatterer such that $2\pi k_F l \gg 1$, where k_F is the wave vector for the electrons at the Fermi-energy, and l is the mean-free path given by $l = \hbar k_F \tau / m^*$. Outside the scattering region the domain is assumed to uniformly extend to infinity.

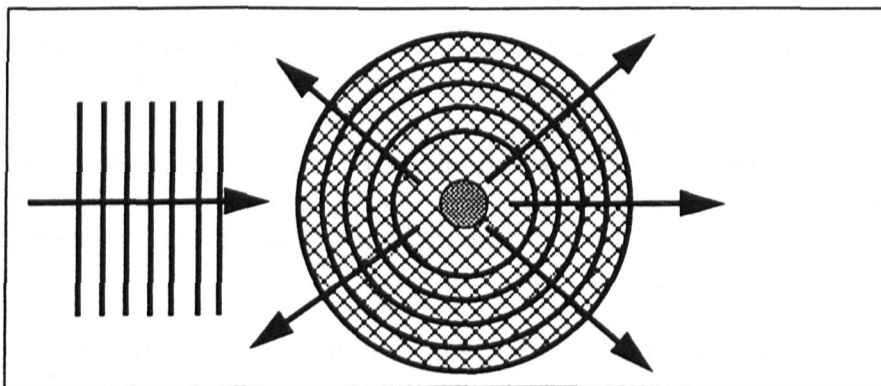


FIGURE 1: A schematic diagram of the 2-D scattering domain with an elastic scatterer at the center. The solution domain is represented by the hatched region.

Within this "jellium" model, the self-consistent electronic states can be explicitly obtained by solving the single electron effective mass Schrödinger equation,

$$-\frac{\hbar^2}{2}\nabla \cdot \left(\frac{1}{m^*} \nabla \psi_E(r, \theta) \right) + [V_R + V_H + V_{SC}] \psi_E(r, \theta) = E \psi_E(r, \theta), \quad (1)$$

where $V_R(r)$ is the potential of the scatterer, V_H is the self-consistent Hartree potential which accounts for many-body Coulombic interactions, and V_{SC} is the electrostatic potential associated with self-consistent screening. Exchange and correlation may also be included within a local density approximation [11]. The z dependence has been dropped by the assumption that only the first subband of the 2DEG is occupied, reducing the problem to circular-polar coordinates.

We assume an incident plane wave of the form $\exp(ik \cdot r)$. The asymptotic solution of this equation in the region where the scattering potential is negligible (the region outside the domain) is given by

$$\psi(r \geq R_0, \theta) = \sum_{m=-\infty}^{\infty} i^m \left[a J_m(kr) + b_m H_m^{(1)}(kr) \right] e^{im\theta}, \quad (2)$$

where we have used the Jacobi-Anger expansion of the incident wave, and J_m is the Bessel function of the first kind with a known incident amplitude a , and $H_m^{(1)}$ is the Hankel function for the outgoing scattered wave with the unknown amplitudes b_m .

Similar to the development of the quantum transmitting boundary method for quasi-1D transport [12], the 2-D transport boundary condition is developed from the orthogonality of the angular modes over the interval $\theta = (0, 2\pi)$, which are used to expand the unknown coefficients, b_m , on the boundary of the domain,

$$b_m = \frac{1}{2\pi i^m H_m^{(1)}(kR_0)} \int_0^{2\pi} e^{-im\theta} \psi(r = R_0, \theta) d\theta - a \frac{J_m(kR_0)}{H_m^{(1)}(kR_0)}. \quad (3)$$

Using this expansion for the b_m coefficients, the normal derivative of the wave-function on the boundary can be obtained,

$$\begin{aligned} \left. \frac{\partial \psi}{\partial r} \right|_{R_0} &= ak \sum_{m=-\infty}^{\infty} i^m \left(J'_m(kR_0) - J_m(kR_0) \frac{H_m^{(1)'}(kR_0)}{H_m^{(1)}(kR_0)} \right) e^{im\theta} \\ &+ k \sum_{m=-\infty}^{\infty} \frac{H_m^{(1)'}(kR_0)}{H_m^{(1)}(kR_0)} \frac{1}{2\pi} \int_0^{2\pi} e^{-im\theta} \psi(r = R_0, \theta) d\theta, \end{aligned} \quad (4)$$

and

$$\left. \frac{\partial \psi}{\partial \theta} \right|_{R_0} = \sum_{m=-\infty}^{\infty} \frac{im}{2\pi} \left(\int_0^{2\pi} e^{-im\theta} \psi(r = R_0, \theta) d\theta \right) e^{im\theta}, \quad (5)$$

where the primes on the Bessel and Hankel functions indicate derivatives with respect to kr . Equations (4) and (5) form the basis for the open 2-D scattering boundary conditions which can be incorporated into the finite element method. It is important to note that the orthogonality of the angular functions requires a circular domain boundary.

III. Numerical Method

The finite element method is used to solve the 2-D effective mass Schrödinger equation on the discretized domain schematically shown by the grided region in Fig. 1. The region

outside the problem domain is assumed to extend to infinity as described in section II. The finite element method is used to linearize the Schrödinger equation, resulting in the weak variational form

$$\begin{aligned} \hat{\mathbf{u}}^T \left(\frac{\hbar^2}{2} \int_{\Omega} \mathbf{B}^T \frac{1}{m^*} \mathbf{B} d\Omega \right) \mathbf{u} + \hat{\mathbf{u}}^T \left(\int_{\Omega} [V(r) - E] \mathbf{N}^T \cdot \mathbf{N} d\Omega \right) \mathbf{u} = \\ \frac{\hbar^2}{2} \int_{\partial\Omega} \hat{\psi} \frac{1}{m^*} \frac{\partial\psi}{\partial r} \Big|_{\partial\Omega} \cdot \hat{n}_{\partial\Omega} d\partial\Omega, \end{aligned} \quad (6)$$

where $\hat{\mathbf{u}}$ is the vector of nodal values for the arbitrary test function $\hat{\psi}$, \mathbf{u} is the vector of unknown nodal values for the wave function ψ , \mathbf{N} is the vector of global orthonormal finite element shape functions, \mathbf{B} is the matrix of spatial derivatives of the \mathbf{N} vector of shape functions, and $\hat{n}_{\partial\Omega}$ is the unit normal to the domain boundary, $\partial\Omega$. The result for the derivative of the wave-function on the domain boundary developed in section II is inserted above to determine the right hand side surface terms. The resulting linear system of equations has the form

$$\hat{\mathbf{u}}^T (\mathbf{T} + \mathbf{V} + \mathbf{C}) \mathbf{u} = \hat{\mathbf{u}}^T \mathbf{P}, \quad (7)$$

where

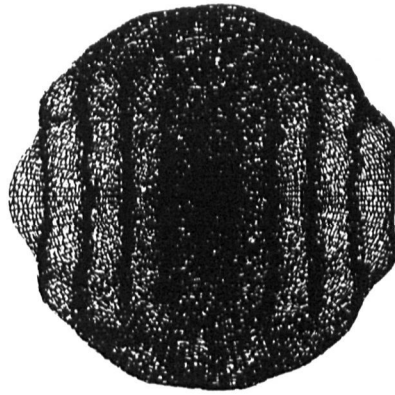
$$\begin{aligned} \mathbf{T} &= \frac{\hbar^2}{2} \int_{\Omega} \mathbf{B}^T \frac{1}{m^*} \mathbf{B} d\Omega \\ \mathbf{V} &= \int_{\Omega} [V(r) - E] \mathbf{N}^T \cdot \mathbf{N} d\Omega \\ \mathbf{C} &= \frac{\hbar^2 k R_0}{4m^* \pi} \sum_{-\infty}^{\infty} \frac{H_m^{(1)'}(kR_0)}{H_m^{(1)}(kR_0)} \left(\int_0^{2\pi} \hat{\psi}(r = R_0, \theta) e^{im\theta} d\theta \right) \int_0^{2\pi} e^{-im\theta} \psi(r = R_0, \theta) d\theta \\ \mathbf{P} &= a \frac{\hbar^2 k R_0}{2m^*} \sum_{m=-\infty}^{\infty} i^m \left(J_m'(kR_0) - J_m(kR_0) \frac{H_m^{(1)'}(kR_0)}{H_m^{(1)}(kR_0)} \right) \int_0^{2\pi} \hat{\psi}(r = R_0, \theta) e^{im\theta} d\theta. \end{aligned}$$

The infinite sums may be truncated to include only the more relevant low angular momentum modes with minimal loss in accuracy. The resulting linear system may be solved by standard LU-decomposition and back substitution using sparse matrix methods for the efficient use of both memory and cpu resources.

IV. A Repulsive Scatterer

Our preliminary results, neglecting electron-electron scattering effects contained in V_H and V_{SC} , are presented for the structure schematically shown in Fig. 1. The infinite repulsive scatterer is centered in the solution domain. The mesh generated for this example contains 10801 nodes connected by 21500 triangular elements. Both skyline storage and bandwidth optimization techniques were employed for an efficient computational solution of the resulting unsymmetric linear system of equations. The real part of the wave function is presented in Fig. 2. The radial and angular modes are clearly visible in the scattered wave.

FIGURE 2: The real part of the scattered wave function for an incident plane wave scattered by a repulsive central field. Both the incident plane wave and the radially scattered contributions are clearly visible. The mesh consists of 10801 nodes with 21500 triangular elements.



V. Summary

We have presented a numerical method to solve the 2-D effective mass Schrödinger equation for an open boundary scattering problem. The method uses partial wave expansion to fully specify the normal derivative of the wave-function on the boundary. The finite element method is used to discretize the Schrödinger equation. The partial wave boundary conditions are used to fully specify the problem which reduces to a linear system of equations which can be solved for the scattering states. The scattering states may then be used to compute the local density of states and the electron density inside the scattering region.

Acknowledgments

This work has been partially supported by the Office of Naval Research and the Air Force Office of Scientific Research. H.K.H. is grateful for a fellowship from the Center for Applied Mathematics of the University of Notre Dame.

References

- [1] R. Landauer, *IBM J. Res. Develop.* **1**, 223 (1957).
- [2] R. Landauer, *Phys. Rev. B* **14**, 1474 (1976).
- [3] C. Bosvieux and J. Friedel, *J. Phys. Chem. Solids* **23** 123 (1962).
- [4] R. S. Sorbello, *Phys. Rev. B* **23**, 5119 (1981).
- [5] R. S. Sorbello, *Phys. Rev. B* **31**, 798 (1985).
- [6] R. S. Sorbello and C. S. Chu, *IBM J. Res. Develop.* **32**, 58 (1988).
- [7] A. H. Verbruggen, *IBM J. Res. Develop.* **32**, 93 (1988).
- [8] M. F. Crommie, C. P. Lutz, and D. M. Eigler, *Nature* **363**, 524 (1993).
- [9] A. Zettl, *Nature* **363**, 496 (1993).
- [10] H. K. Harbury, W. Porod, C. S. Lent, *Superlat. Microstruct.* **11**, 189 (1992).
- [11] Y. Sun and G. Kirczenow, *Phys. Rev. B* **47** 4413 (1993).
- [12] C. S. Lent and D. J. Kirkner, *J. Appl. Phys.* **67**, 6353 (1990).